Helicity Injection and Dissipation in the Edge Region on a Reversed Field Pinch

SHINOHARA Shunjiro

Department of Physics, Faculty of Science, University of Tokyo

Reprinted from

Journal of Plasma and Fusion Research

Vol. 70, No. 11 (1994), pp. 1182~1195.

研究論文

Helicity Injection and Dissipation in the Edge Region on a Reversed Field Pinch

SHINOHARA Shunjiro*

Department of Physics, Faculty of Science, University of Tokyo, Tokyo 113, Japan.

(Received 11 April 1994/revised manuscript: received 8 September 1994)

Abstract

Helicity injection and dissipation in the edge plasma region are studied in the REPUTE-1 reversed field pinch (RFP) device. Increases in one-turn loop voltage V_l and magnetic fluctuations with nearly constant ion temperature are found advancing movable limiter or injection probe into the plasma. A drastic increase in V_l is observed with an insertion of ~ 8cm from the plasma edge. This V_l increase under various conditions is discussed comparing with theories. The induced voltage between parallel plates (poloidal direction) is measured (< 60V) as a function of the insertion depth, which shows the presence of the high energy electrons (at least more than 20eV with a relative population of less than several %).

The first dc helicity injection is tried applying a voltage between two parallel plates (injection probe) inserted to the plasma edge, and effects on plasma performance are studied. The injected current up to 9kA is nearly proportional to the applied voltage V_H with a small offset voltage. A transient increase in the toroidal flux by ~ 10% and a decrease in the poloidal field by < 10% are found (plasma takes the more relaxed state) near the injection port, regardless of the polarity of V_H. An analysis of electrical circuit is also done to estimate the load of the probe part.

Keywords:

RFP, plasma edge, dissipation, helicity, relaxation, injection, PWI,

1. Introduction

Reversed Field Pinch (RFP) [1] is characterized by comparative toroidal and poloidal magnetic field components which form nested flux surfaces with low safety factor, high shear and high beta value. This, a class of toroidal plasma confinement device, gives us the interest in plasma physics such as a magnetic relaxation process constrained by magnetic helicity conservation in addition to the anomalous heating and anomalous resistance [2]. In current-carrying toroidal devices, a method of continuously driving the toroidal current is necessary for steady-state operation [3,4]. The basic idea is to inject "helicity" into the plasma based on the Taylor's principle [5], and a recent trial of ac or dc helicity injection may lead to more efficient methods of this operation [6-8]. The relaxation process during this injection is also a major concern in RFP because there exists a nonlinear response such as a dynamo activity [1]. Recently, a simulation study [9] has been done to demonstrate a suppression of the MHD instabilities by dc injection in RFP. Although a helicity injection scheme may be an important potential tool to the

Present Address: Interdisciplinary Graduate School of Engineering Sciences, Kyushu University, Kasuga 816, Japan.

current drive and MHD stabilization in RFP, as far as we know, only one first trial was reported [10] to change the plasma properties by the dc helicity injection.

In studying the helicity injection, plasma-wall interaction [11] can be an important factor to the plasma dissipation near the plasma edge, when the material is inserted into the plasma edge region. Even if the injection scheme is promising, this interaction may mask this injection effect when the deterioration of the plasma is evident. In addition, edge conditions govern the plasma behaviors such as impurities, plasma parameters and confinement. This insertion may also be connected with the anomalous resistance and anomalous heating [2], which are considered to be related with the dynamo activities. As for the movable limiter insertion experiments [12-17], increases in a loop voltage and the ratio of ion to electron temperatures are found, but other plasma parameters (except for CV line intensity and edge radiated power) have not been measured fully. Although some theories are presented from helicity conservation [14,18] and kinetic dynamo models [19], these phenomena observed have not yet been fully interpreted. In addition, basic experimental data, namely shape of movable limiter, material, plasma parameters obtained etc., are not enough.

Here, we present the experimental results on the deep (up to half minor radius) insertion of material objects (movable limiter and injection probe), from a view point of the edge plasma dissipation in the RFP machine, REPUTE-1 [20] (major and minor radii are $R = 82$cm and $a = 22$cm, respectively). Measurements of magnetic fluctuations and intensities of soft X-ray and H_α are newly added to other measurements. Next we report the experimental results on the dc helicity injection, in the form of the product of the electrostatic potential difference and the magnetic flux. This injection is the first trial to see the effects on the global plasma performance in connection with the relaxation phenomena. Furthermore, we try to check whether this injection affects the impurity production or not due to the plasma-surface interaction [17,21,22], including hot energy electrons [23-27] near the plasma boundary by inserting a injection probe.

In Sec.2, we show the experimental results, *i.e.*, changes of plasma parameters as a function of material insertion depth, by using various types of movable limiter and injection probe after describing their configurations. A discussion on this increase in the loop voltage is also presented, comparing with theories based on the resistivity and helicity. Presence of high energy electrons is also discussed, considering the observed induced voltage. In Sec.3, effects on plasma performance in the helicity injection trial is reported after describing a characteristics (setup and electric circuit) of an injection probe. Finally, conclusions are presented in Sec.4.

2. Material Insertion

2.1 Change of Plasma Parameters

In the previous paper [15], we have shown the slight increase in the one-turn loop voltage V_l as the movable limiter moves into the plasma in the REPUTE-1 RFP device. In addition, the increasing rate of V_l is weakly dependent on the rotation angle of the limiter plate with respect to the magnetic field line.

In order to see the effects on plasma performance, we use various types of movable limiter and injection probe [10,17], *i.e.*, mainly four types as follows: 1) a rectangular solid made or ceramic (macor), 1.18cm high (poloidal direction) and 2.08cm wide (toroidal direction) with 20cm length (radial direction) (two stainless steel plates, 0.3cm thick and 1.48cm wide, are put into the top and bottom sides) (type A, shape is similar to type B in Fig. 7 in the helicity injection case), 2) a larger size of type A, namely 1.18cm high and 2.98cm wide with 20cm length (also two stainless steel plates, 0.3cm thick and 2.38cm wide, are located into the top and bottom sides) (type B, see also Fig. 7), 3) a disc, 2.5cm in diameter with 0.4cm thickness (radial direction) made of stainless steel, connected with a circular cylinder (1.4cm in diameter made of Boron Nitride with 24cm length (radial direction)) (type C), 4) a stainless steel plate, 3.5cm wide (toroidal direction) and 10cm high (poloidal direction), with 0.3cm thickness (radial direction) and a macor plate with the same size on the back of it, connected with a circular cylinder (1.2cm in diameter made of macor) (type D). These (types A to D) are inserted

into the plasma from the side port in the REPUTE-1 device.

By rotating types A and B (by the use of rotation mechanism at the other end of the probe in Fig. 7) to change the angle between their heads and magnetic field line, *i.e.*, metal plates can see the plasma from poloidal to toroidal directions, plasma parameters change only slightly. The data shown here are obtained by the type A unless mentioned. Typical plasma parameters analyzed here at the time of the plasma current peak are the followings; plasma current $I_p = 200$kA, one-turn loop voltage $V_l = 180$V, mean (line averaged) plasma density $\bar{n}_e = (3\text{-}4) \times 10^{13}$cm^{-3}, toroidal flux $\Phi = 0.013$Wb, F and Θ are around (0.4-0.5) and 2-2.2, respectively (see Fig. 1). Here, F and Θ are the toroidal and poloidal fields at the plasma edge normalized by the mean toroidal field, respectively. For the case of material insertion, the capacitor charging voltage of the ohmic power supply is increased by less than a few % to maintain the plasma current of 200kA.

Figure 2(a) shows a relationship between loop voltage V_l at the time of the maximum plasma current ($t \sim 0.8$ms for no insertion case) and the insertion depth D from the plasma edge (wall). With an advance of this material into the plasma, an increase in V_l is found. The drastic increase in this V_l around 8cm is coincided with the abrupt

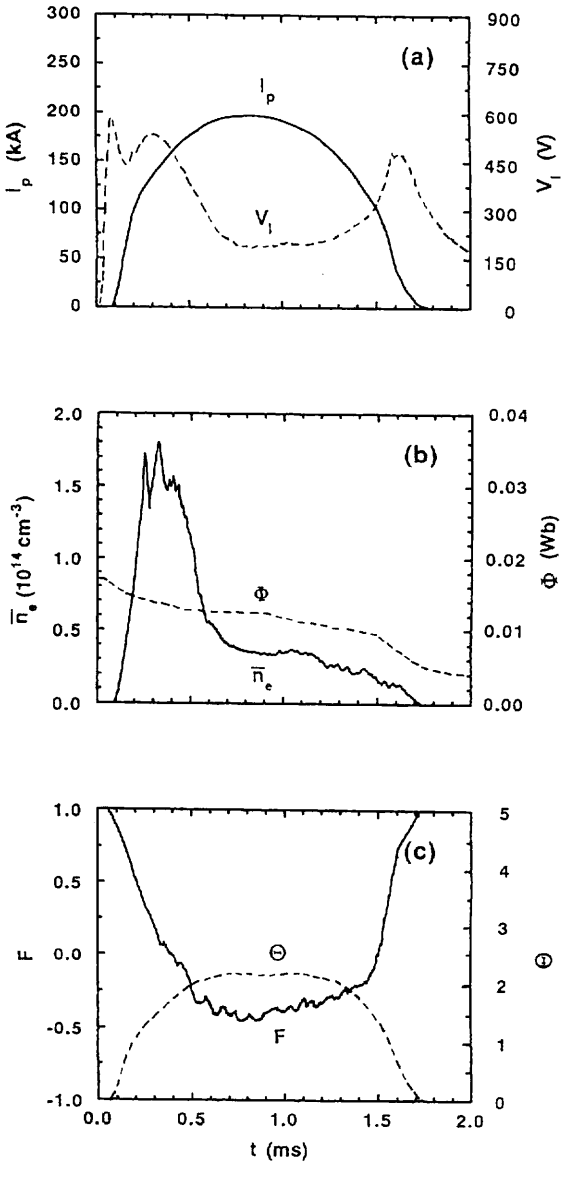

Fig. 1 Typical waveforms of plasma current I_p and one-turn loop voltage V_l (a), mean plasma density $\bar{n}_e$ and toroidal flux Φ (b), and F and Θ (c).

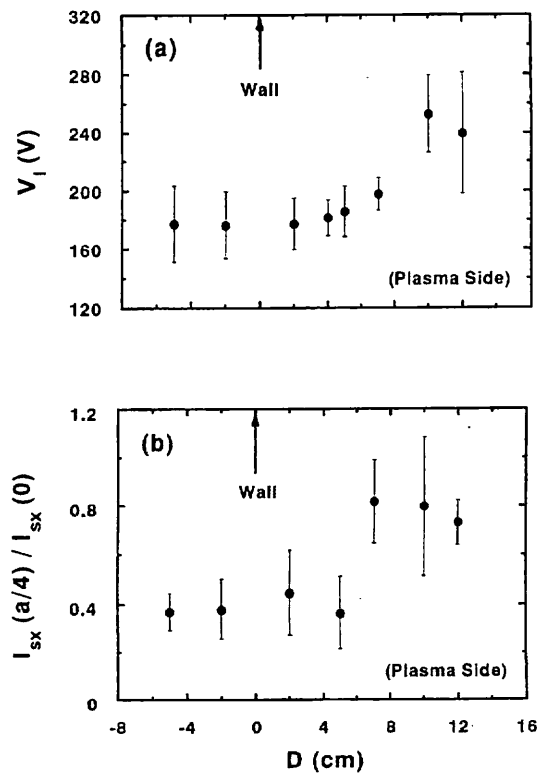

Fig. 2 One-turn loop voltage V_l (a) and ratio of soft X-ray intensity I_{sx} $(a/4)/I_{sx}$ (0)(b) vs. insertion depth D.

increase in the soft X-ray intensity ratio $I_{sx}(a/4)/I_{sx}(0)$, as shown in Fig. 2(b). This is measured at the chord radius of $a/4$ and at the plasma center by surface barrier diodes ($\phi = 60°$ with ϕ is the toroidal angle from the port of material insertion) [28]. The icrease in this ratio comes mainly from the $I_{sx}(a/4)$ rise, which may indicate the increased impurity radiation. At least the increases in the central electron temperature and mean plasma density are not found from measurements. (Of course, the hot electron contribution must be also considered.) These obtained dependencies are inherent characters of the material object insertion (without any active function), because the observed results were completely different when we use the pump limiter head (active function) [17].

These results of drastic increases in V_l and the ratio, $I_{sx}(a/4)/I_{sx}(0)$, may affect the core (the inside region of the plasma, more than 8cm from the plasma edge) confinement. The increasing rate of V_l as a function of the insertion depth D ($D < 5$cm) is nearly the same order with the previous REPUTE-1 result [15] as well as the HBTX1 [12-14] and ZT-40M [16] ones.

Although the increase in the loop voltage is observed, the ion temperature T_i derived from Doppler broadening of CV line (wavelength $\lambda =$ 227.1nm, $\phi = 40°$) does not change very much, as shown in Fig. 3. The result of the nearly constant ion temperature with an insertion up to 12cm, which is beyond the half of the minor radius of 22cm, is observed for the first time in RFP experiments.

On the other hand, the central electron temperature T_e by Thomson scattering ($\phi = -120°$) shows a tendency to decrease slightly with the insertion depth D (Fig. 3). The intensities of H_α ($\phi = 180°$), CV and soft X-ray gradually decrease with D ($D < 9$cm). Note that the data are taken at the same time in this device for the same value of D, and obtained results (dependence on D) are nearly the same if we normalize respective plasma parameters by the mean plasma density.

As for magnetic fluctuations measured by magnetic probes ($\phi = 19°$) located on the inner wall of the torus [29], similar changes with V_l are found by material insertion, as shown in Fig. 4. Here, the amplitude (root mean square) is derived near the

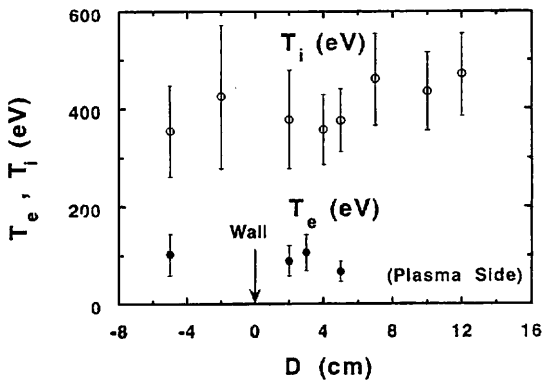

Fig. 3 Ion temperature T_i (open circles) from CV Doppler broadening and central electron temperature T_e (closed circles) by Thomson scattering as a function of insertion depth D.

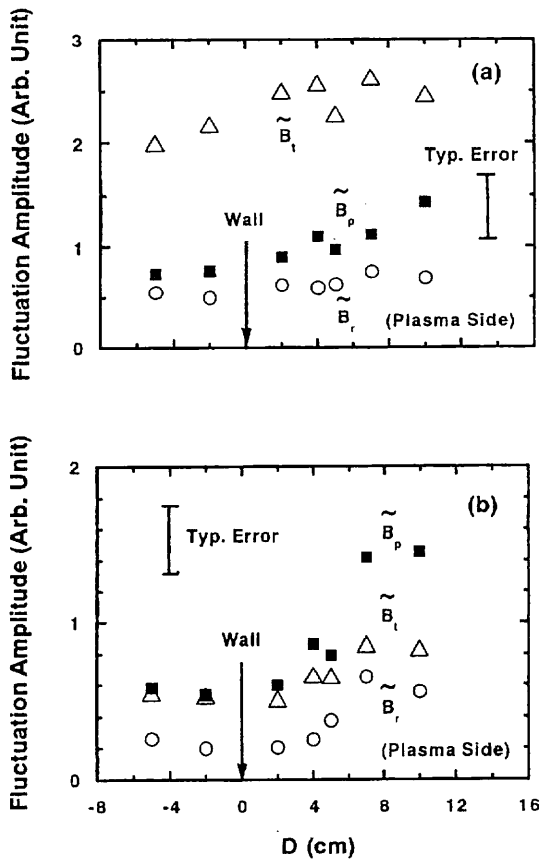

Fig. 4 Fluctuation amplitudes (root mean squares) of toroidal (B_t, open triangles), poloidal (B_p, closed boxes) and radial (B_r, open circles) components of magnetic fields vs. Insertion depth D for the lower (5-50kHz)(a) and the higher (50-200kHz) (b) frequency ranges.

time of the maximum plasma current for 0.2ms time window (sampling time is 2μs). Three components of B_t (toroidal), B_p (poloidal) and B_r (radial) fields are measured, and an averaging of two signals, detected at the inner and outer equators, has been done for each component. In addition, two numerical (band pass) filters of 5-50kHz (lower frequency, LF) and 50-200kHz (higher frequency, HF) are used for comparison. The increasing rate of fluctuations of three components is higher for the HF range than that for the LF one.

2.2 Discussion on the Voltage Increase

The increasing rates of V_l as a function of D (D < 4cm) obtained in the REPUTE-1 are roughly ~ 3V/cm, 3-4V/cm, ~ 3V/cm and 5-6V/cm for types A, B, C and D, respectively. Previous result [15] showed ~ 1V/cm for the case of a stainless steel plate, 0.3cm thick and 3.5cm wide. There is a tendency that a rod type as well as a rectangular solid type raise the increasing rate of V_l higher than a plate type.

Hereafter, the loop voltage increase is examined and compared with theories. First the classical (Spitzer) resistivity is considered. When we take an experimental value of V_l = 180V without a limiter insertion and assume the spatially uniform resistivity, $\Delta V_l/D$ ~ 9V/cm can be expected if a plasma diameter diminishes with the same rate of the insertion depth. This value is large compared with four cases mentioned above, which indicates existences of (i) a non-Spitzer resistivity part, (ii) non-uniform resistivity profile, (iii) smaller limiter effect to reduce the plasma radius and (iv) a decreased resistivity. The last one of (iv) does not explain the results due to the facts that the central electron temperature does not change very much (at least does not increase) and intensities of CV line and soft X-ray do not decrease appreciably by the insertion. Now we check three reasons of (i)-(iii).

(i) The one-turn loop voltage is considered to be divided into a Spitzer resistivity part and non-Spitzer one [1]. From the modified Bessel function model to analyze the RFP equilibrium [30], the non-Spitzer part is estimated to be ~ 30% of the observed voltage in the REPUTE-1. If we treat that the voltage increase comes from the change of the Spitzer resistivity part due to a reduction of plasma size, then $\Delta V_l/D$ = 9V × 0.7 ~ 6V/cm can be expected, which may explain the experimental results.

(ii) If the plasma resistivity is not uniform (higher near the plasma edge than the inner region), $\Delta V_l/D$ ~ 9V/cm must be lowered; Assuming a resistivity is proportional to $\{c(1-x^2)^m + (1-c)\}^{-3/2}$, $\Delta V_l/D$ are 0.8 and 1.7V/cm for c = 0.9 and 0.8 (m = 1), respectively. Here, we use the parabolic electron temperature profile with a pedestal of (1-c), and constant z_{eff} (effective charge) is assumed (x is a normalized plasma radius). For the case of the broader temperature profile (m = 0.5), $\Delta V_l/D$ are 1.5 and 2.2V/cm for c = 0.9 and 0.8, respectively. This situation may cause an under estimate value, because taking off only the low temperature edge region is hard to be realized.

(iii) The smaller material size can be interpreted to have a smaller limiter effect on the plasma radius reduction, which is consistent with the experimental phenomena described above.

These three reasons combined are plausible to explain the data. Several years ago, we removed the fixed limiters to increase the plasma radius from 20 to 22cm and a reduction of the loop voltage was found (roughly from ≤ 220V to ~ 180V). This voltage is nearly inverse proportional to the cross section of the plasma. This means $\Delta V_l/D$ ≤ 10V/cm (also the plasma resistance without a limiter insertion obeyed roughly − (3/2) power law of I_p [15]) and suggests that the loop voltage is mainly governed by the Spitzer resistivity.

Next, we discuss the voltage increasing rate from theories based on the helicity dissipation at the plasma boundary. According to Ref.14, the increasing rate of V_l is $\Delta V_l/D = \Delta\chi w(\Theta/\pi a^2)$ ~ 0.06V/cm if we use the value $\Delta\chi$ (potential difference between the points of exit and entry of the field lines) = 15V, w (limiter width in the toroidal direction) = 1cm and Θ = 2. In order to explain the experimental data, $\Delta\chi$ or a projection area wD must be multiplied by a factor of several tens. In addition, the voltage increase obtained is not proportional to the projection area. For the plasma shift case [14] (a displacement of plasma column by the external vertical field), $\Delta V_l/D$ =

$\Delta\chi$ $(4R\Theta/a^2)$ is calculated to be ~ 20V/cm, which is larger than the data by several times.

The paper in Ref.18 claims that V_l is determined by the edge volume region V_e as defined by the limiters, field errors and a plasma shift: $\Delta V_l/D = (E_{//}\Theta/\pi a^2)\ V_e/D$ ($E_{//}$ is parallel dynamo electric field). If we take $\Theta = 2$ and a width of edge region of 1cm for example, $\Delta V_l/D$ is roughly ~ 130V/cm, which is also larger than the experimental values by more than one order of magnitude. Here, a width of 1cm is a distance between the inner edge of the liner and a pedestal for mounting the fixed limiters. In this calculation, we assume that a resistivity part in the bulk plasma is much smaller than the edge plasma dissipation part [18] ($E_{//}$ becomes ~ 2V/cm in the REPUTE-1). Even if we take the width of several centimeters, $\Delta V_l/D$ is still larger than the obtained values by nearly a factor of ten.

Table 1 summarizes the comparison between the various experiments and theories. From the discussion above, it is somewhat difficult for adopting the concept of the helicity balance [18] and the surface term [14] to explain the results quantitatively in the REPUTE-1 (Only if the edge plasma dissipation part is much smaller than a bulk resistivity part, *e.g.*, less than a few %, the theory [18] may account for the experimental results). An electron momentum diffusion to the plasma edge [19] may explain the anomalous loop voltage partly [25-27,31]. However, applying this theory to the voltage increase is out of scope owing to a difficulty to evaluate the theoretical value as is also mentioned in that paper. Basically the effective reduction of the plasma size can be a candidate for explaining the obtained results. The smaller material size can be interpreted to have a smaller effect on the plasma radius reduction. Of course, it can not be excluded partly that V_l increases with an material insertion due to an increase in the impurity contents.

2.3 Analysis of Non-Zero Induced Voltage

When the two parallel plates, facing the poloidal direction like type B probe (see Fig. 7), are inserted into the plasma without connecting with the power supply, the induced non-zero voltage V_P between the plates appears. Note that V_H measured at the feedthrough position is considered to be the same with V_P as the probe current I_H is zero. Here, the positive V_H is defined such that the electron drift side (along the poloidal filed) is positive with respective to the ion drift side. Experiments have been executed under the same plasma conditions is Sec.3 unless mentioned. Note

Table 1 Comparison of loop voltage increasing rate $\Delta V_l/D$ between experiments and theories for I_p~200kA case (ΔV_l: increment of one-turn loop voltage, D: insertion depth from wall).

[1. Experiment]	V/cm	Remark
Type A	~ 3	Material Insertion
Type B	3 - 4	Material Insertion
Type C	~ 3	Material Insertion
Type D	5 - 6	Material Insertion
Previous Movable Limiter	~ 1	Ref. 15 (S. Shinohara *et al.*)
Change of Plasma Size	≤ 10	From a = 20 to 22 cm
[2. Theory]		
Reduction of Plasma Radius	~ 9	Constant Resistivity
Same with Above	~ 6	Spitzer Part Only
Reduction of Plasma Radius	< 9	Hollow Resistivity Profile
$\Delta\chi$ w $(\Theta/\pi a^2)$	~ 0.06	Ref. 14 (H. Y. W. Tsui)
$\Delta\chi(4R\Theta/a^2)$	~ 20	Same with Above (Plasma Shift)
$(E_{//}\Theta/\pi a^2)V_e/D$	~ 130	Ref. 18 (T. R. Jarboe & B. Alper)

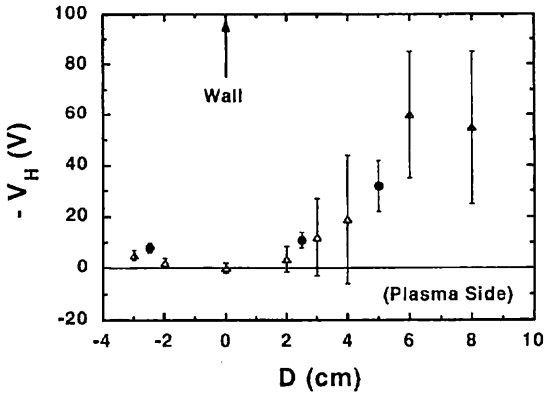

Fig. 5 Induced voltage difference between two plates $-V_H$ as a function of the insertion depth D without an injection (error bars show the root mean square fluctuation levels). Closed circles and open triangles represent cases of plasma current I_P = 130kA and 200kA, respectively.

that the central electron temperature is less than 50eV for $I_P = 130$kA case.

Figure 5 shows V_H as a function of insertion depth D for the two different plasma current cases at the time of this current peak of $t \sim 0.65$ms (V_H does not differ very much compared with that at t = 0.4ms analyzed in Sec.3). With an advance of the probe head into the plasma, we can see the rise of $|V_H|$. The mean voltage itself is not different between two cases, but the fluctuating amplitude is larger for the higher current case of $I_P = 200$kA. The non-zero voltage of V_H can be explained partly by the high energy electrons [23-27]. We define $\alpha = n_h/n_e$, $\beta = v_d/v_{the}$, and $\gamma = v_h/v_{the}$ (n_h: density of high energy electrons, n_e: plasma density, v_d: drift velocity of the bulk electron plasma, v_{the}: electron thermal velocity, v_h: velocity of high energy electrons). The voltage V_H (floating potential difference between ion and electron drift sides of the probe) is calculated under the condition that the sum of the ion saturation current and electron current is zero for both sides. Here, we use a drifted Maxwellian distribution of bulk electrons with $T_e = 7$eV and a half Maxwellian distribution of hot electrons (α, β and γ are free parameters to match the experimental value).

If there are no high energy electrons of $\alpha = 0$, the value of β must be larger than one, as shown in Fig. 6 (a) (voltage difference $\Delta V = -V_H$ is only

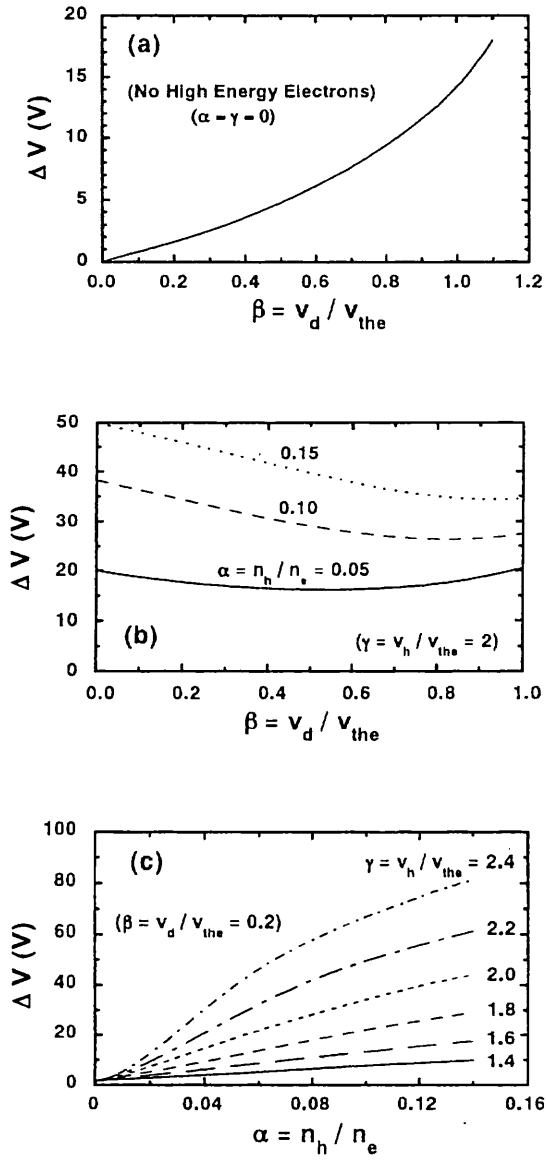

Fig. 6 Calculation of voltage difference ΔV between two plates as a function of β with $\alpha = \gamma = 0$ (no high energy electron) (a), β with $\gamma = 2$ (α is a parameter) (b) and α with $\beta = 0.2$ (γ is a parameter)(c).

14V even for high normalized drift velocity of β = 1). This means that non-zero values of α and γ are needed (presence of high energy electrons) in order to explain the data in Fig. 5 quantitatively. The V_H value is weakly dependent on β (*e.g.*, see Fig. 6 (b)), so we take $\beta = 0.2$ for convenience (*e.g.*, $\beta = 0.11$-0.22 when we use $j = 20$-40A/cm^2, $n_e = 10^{13}$cm^{-3}

and $T_e = 7$eV). In this case, we have, for example, $\alpha = 0.04$ with $\gamma = 2.4$ (high energy electron temperature $T_{eh} = 40$eV) and $\alpha = 0.085$ with $\gamma = 2.0$ ($T_{eh} = 28$eV) for $V_H = -30$V case, as shown in Fig. 6(c). When γ is less than 1.8 ($T_{eh} < 23$eV), α must be larger than 0.15, which is unlikely to occur. On the other hand, when γ are greater than 2.5 ($T_{eh} > 44$eV) and 3.5 ($T_{eh} > 86$eV), α become lower than 3% and 1%, respectively; With a decrease in α, γ and thus T_{eh} become higher for a fixed β value. From this, we need, roughly, high energy electrons of (at least more than 20eV) with a relative population of less than several %. This result is consistent with experimental results by thermocouples [27] and an electron energy analyzer [26], and also with an estimation [25] in the REPUTE-1 device: T_{eh} is roughly an order of the central elctron temperature with a relative population of less than several %.

3. Helicity Injection

3.1 Current Injection

The exprimental set-up including an injection probe is shown in Fig. 7 (same with type B), using the same port in Sec.2: two stainless steel plates facing the poloidal direction, are put into on both sides of the rectangular solid (macor). Two plates of this probe, which is rotatable (*e.g.*, it is possible to face the toroidal direction), are connected to the power capacitor bank (11.2mF with 1.9kV maximum charging voltage) through a resistance $R_C \sim 30\ m\Omega$ and an inductance $L_C \sim 60\mu$H by a thyristor switch. Typical target plasma parameters analyzed here are, plasma current I_P is 130kA, mean plasma density $\bar{n}_e$ is (3-4) $\times 10^{13}$cm^{-3}, F and Θ are around-(0.2-0.4) and 1.8-2, respectively. The discharge duration time is $\sim$ 1.3ms and the time of the maximum plasma current is $\sim$ 0.65ms.

In this experiment, the injected current starts at $t = 0.2$ms (plasma is initiated at $t = 0$ms) and the time to reach the maximum current is $\sim$ 1.2ms (time evolution of injected current is shown in Fig. 9). The obtained data are taken under the condition that the head of the injection probe is inserted to $D = 5$cm typically from the wall (outer side of the torus). For the case of $D < 5$cm, the change of plasma parameters by the injection are reduced compared with $D = 5$cm case. For $D \leq 2$cm case, the probe current I_H is unsettled (I_H differs from shot to shot) and a further insertion of

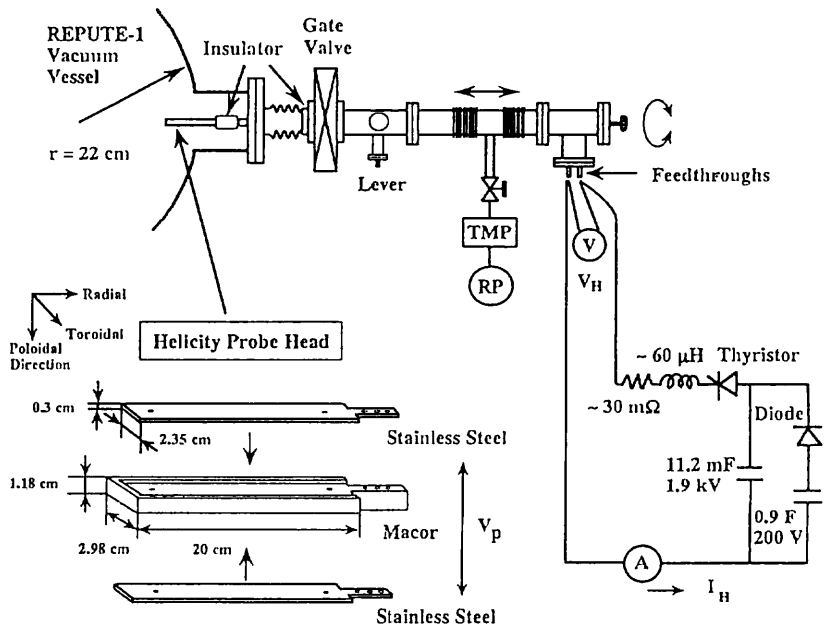

Fig. 7 Experimental set-up for dc helicity injection.

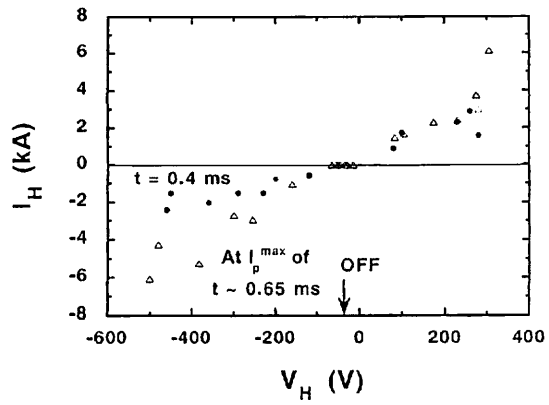

Fig. 8 Relationship between injected current I_H and applied voltage V_H between two plates at t = 0.4ms and near the time of the maximum plasma current I_p^{max}.

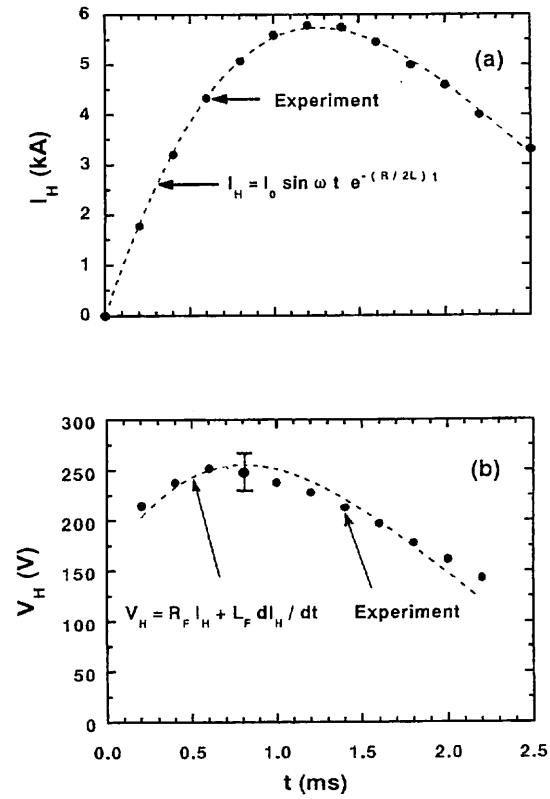

Fig. 9 Time evolutions of the injected current I_H (a) and applied voltage V_H (b) with the capacitor charging voltage of V_0 = 1kV (t = 0ms means 0.2ms after plasma initiation). Here, closed circles and dotted lines show the data from experiments and calculation, respectively, and error bars show the experimental fluctuation amplitudes of V_H.

D > 5cm degrades the plasma behaviors described in Sec.2. The obtained current I_H is nearly proportional to the applied voltage V_H between two parallel plates (measured at the feedthrough position) for individual time, *e.g.*, $|I_H| \sim$ 2kA at t = 0.4ms and $|I_H| \sim$ 3kA at t = 0.65ms for $|V_H|$ = 300V case, as shown in Fig. 8. The maximum I_H obtained, which is limited by the damage of the injection probe, is ~ 9kA (t = 1.4ms) with an initial charging voltage V_0 of the capacitor is 1.6kV (this maximum I_H is also proportional to V_0). Note that obtained current is very high compared with estimated currents of the ion and electron saturation, ~ 24A and ~ 1kA, respectively. Here, we use the electron density $n_e = 10^{13}\text{cm}^{-3}$ and electron temperature T_e = 7eV assuming no sheath region near the probe. Although some thin scratches and erosions on the stainless steel plates are observed, the suface of the macor is relatively clean with no distinct tracks after the experiments.

From the analysis of the waveform measurements of the circuit current I_H and the voltage V_H as shown in Fig. 9, we can estimate the electric circuit values. When I_H is expressed as $I_0 \sin(\omega t) \exp(-Rt/2L)$, total inductance L of ~ 99μH and resistance R of ~ 95mΩ are obtained from the data in Fig. 9(a) ($I_0 = V_0/L\omega$, $\omega^2 = 1/LC - R^2/4L^2$,$C$: capacitance). Here, we assume that R, L and C are series connected. The waveform of V_H, as shown in Fig. 9(b), expressed as $R_F I_H + L_F dI_H/dt$ leads to $R_F \sim$ 41mΩ and $L_F \sim$ 16μH by fitting the data (R_F and L_F are taken from the probe tip, including probe load part, to the feedthrough position. In these calculations, constant circuit values are assumed, which can well fit the experimental data, as shown in Fig. 9(a) and (b). After subtracting the value between the feedthrough and probe, *i.e.*, feeder part, the effective resistance and inductance, of the load (only probe part) can be estimated roughly as R_H ~ 30mΩ and $L_H \sim$ several μH, respectively. Note that we can calculate that $R_H \sim$ 44mΩ and $L_H \sim$ 0.92μH if the current path in the plasma is an annular structure (one turn), 126cm long (radius of 20cm) with a cross section of Δr (radial length) = 5cm and Δz (toroidal length) = 2.35cm, and T_e = 7eV with z_{eff} = 1. At the plasma current maximum of $t \sim$ 0.65ms, a ratio of probe voltage V_P (just between two parallel plates) to V_H is estimated to be

$\sim$ 0.5.

Three components (toroidal, poloidal and radial directions) of edge magnetic fields at ϕ (toroidal angle from the injection port) = 19° [29] show that the fluctuation levels of low (5-50kHz) and high (50-200kHz) frequencies do not show appreciable changes due to mainly, the relatively large scatters (statistical large error bars) of the data, varying V_H. On the contrary, low frequency parts of I_P ($\phi = 127°$) and one-turn loop voltage V_l increase slightly with $|V_H|$.

The mean density j_ϕ with the plasma current I_P = 130kA is 85A/cm^2. Here, I_P is nearly the same with the estimated total poloidal current from equilibrium calculation, using F and Θ values. When we take the surface area as the probe surface (Δr = 5cm and Δz = 2.35cm), the mean injected current j = 255A/cm^2 for I_H = 3kA. In this experiment typically, the relative helicity injection rate $V_P B_P S / V_l \Phi$ is 1.3% (B_P: poloidal field, S: surface area of the injection probe facing the plasma poloidally, Φ: toroidal flux), and the relative ohmic injection rate $V_P I_H / I_P V_l$ is 2%.

According to Ho [9], we need that the total injected current I_H is an order of I_P and the relative injection rate is serveral tens of % (and also injected current density j is greater than j_ϕ especially at $r \sim 0.8a$) to stabilize the MHD instability (current driven mode). This shows that the experimental values of injection rate and current seem to be low to have this stabilizing effect. The effects such as the current diffusion may lower the injected current density in the plasma. Note that this density may be larger than j_ϕ near the injection port locally.

3.2 Plasma Performance

Here, we report the changes of plasma parameters by this dc injection. Figure 10 shows a relative increase in the toroidal flux near and far from the injection port ($\phi = -55°$ and 130°, respectively) as a function of V_H at t = 0.4ms. From this figure, we can see that the flux increase up to $\sim$ 10% is independent of the polarity of V_H and that the increase is localized near the injection port. There is a tendency that this flux increase saturation with $|V_H|$. However, this increase reduces at the time of the plasma current peak even near the injection port: time evolution of the toroidal

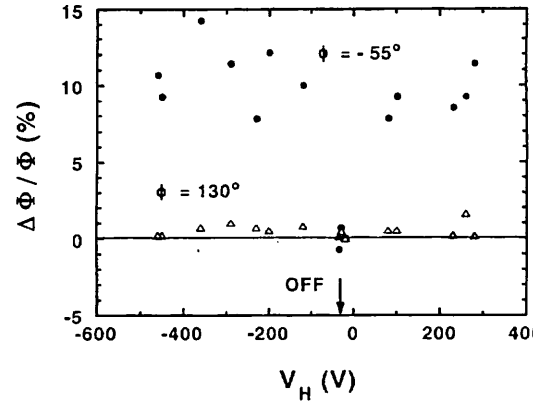

Fig. 10 Relative changes of toroidal flux $\Delta\Phi/\Phi$ near ($\phi = -55°$, closed circles) and far ($\phi = 130°$, open triangles) from the injection port as a function of applied voltage V_H at t = 0.4ms.

flux exhibits a "hump" near the time of t = 0.4ms. The reason why the voltage $|V_H|$ is not zero, *i.e.*, ~ -30V when the power supply is off (without an injection) is due to the presence of the high energy electrons, which has been discussed in Sec.2.3. Rotating this injection probe by 90° (two parallel plates face toroidal direction) leads to the same trend of the transient increase in the toroidal flux near the injection port (dependence of I_H on V_H is also similar). Note that the ratio of helicity injection in the toroidal to poloidal directions is $V_P B_t S / V_P B_P S \sim B_t / B_P \sim |F/\Theta| \sim 0.1 - 0.2$. By

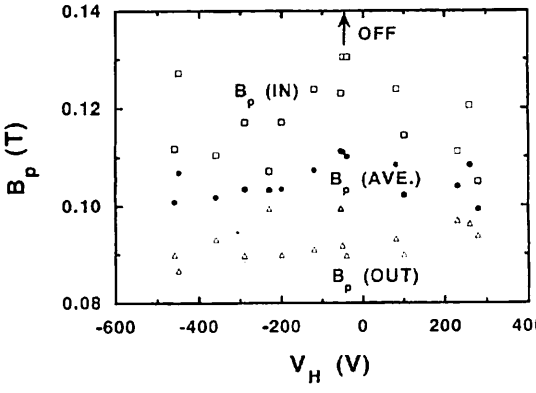

Fig. 11 Relationship between edge poloidal fields B_p (ϕ = 19°) and applied voltage V_H at t = 0.4ms. Here, open boxes, open triangles and closed circles show the poloidal fields measured at the inner and outer sides of the torus, B_p (IN) and B_p (OUT), and the average field B_p (AVE.), respectively.

increasing I_P from 130kA to 200kA, this flux change reduces due to mainly the decrease in the relative injection current I_H/I_P and the enhanced plasma-probe interaction.

In addition to the change of the toroidal flux, the edge poloidal field B_P is somewhat modified by this injection, as shown in Fig. 11. Here, this field is measured at $\phi = 19°$ [29] ($t = 0.4$ms), and the average B_P (two signals at the inner and outer equators are averaged) decreases gradually by $< 10\%$, which suggests the broadening of μ profile (ratio of the current density to the magnetic field), also regardless of the polarity of V_H. The edge toroidal field, also measured at $\phi = 19°$, decreases slightly at $t = 0.4$ms for $V_H > 0$. From the soft X-ray measurements by the surface barrier diodes ($\phi = 60°$) [28] with an injection, the increase in this intensity is more at the outer chord ($r = 12$cm) of the plasma compared with the central chord. This shows that the injection affects more at the outer region of the plasma. However, the impurity intensities such as CV and OV (mainly emitted from the central plasma region and from the inner plasma region, respectively, $\phi = 40°$) do not increase appreciably with V_H (the H_α intensity at $\phi = 180°$ does not change either). Even though a small increase in V_l is observed with an insertion of $D \leq 5$cm described in Sec.2.1, the degradation of the plasma properties are not found for the case of the injection.

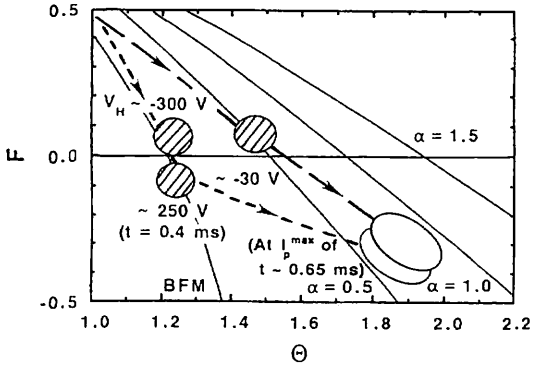

Fig. 12 Time evolution of F-Θ trajectories with (near the injection port, dotted line) and without (dashed line) helicity injection. Here, shaded area are taken at $t = 0.4$ms (for three cases of $V_H \sim -300$V, ~ -30V (without injection) and ~ 250V) and open areas near the time of the maximum plasma current I_p^{max} ($t \sim 0.65$ms). For comparison, theoretical curves from BFM (Bessel Function Model) and from the μ profile (index of α is indicated) with poloidal beta value β_p of 0.1 are also shown.

If we can combine the data of the toroidal flux at $\phi = -55°$ (Fig. 10), the average poloidal (Fig. 11) and toroidal fields at $\phi = 19°$, F and Θ values near the injection port can in principle be derived. This means a breaking of the toroidal symmetry, opposing the generally accepted RFP equilibrium description. However, here we define local F and Θ values for convenience from a view point of a localized effect. Figure 12 shows the time evolution of F-Θ trajectories near the injection port, with and without this injection. Note that the general F-Θ trajectory with an injection (far from the injection port) is nearly the same with the one without an injection. Here, shaded area are taken at $t = 0.4$ms (for three cases of positive, negative applied voltages and no injection) and open areas are at ~ 0.65ms (at the time of the maximum plasma current I_P^{max}). Curves from the Bessel function model (BFM) [1] and modified Bessel function model [30] are also shown for comparison; Poloidal beta value of β_P is 0.1 with α is a parameter to express the μ profile as being proportional to $\{1 - (r/a)^2\}^\alpha$. Note that the increase in β_P causes the theoretical curves to the right side region (Θ increases with the same F value). With an injection, plasma takes the broader μ profile regardless of the polarity of V_H, *i.e.*, more relaxed state (near the BFM curve) at $t = 0.4$ms. This effect fades away as time goes on (shifts to the right region of more peaked μ profile).

It is interesting but not certain why the plasma response is nearly the same regardless of the polarity of V_H and also nearly the same by rotating the probe by 90°. As stated before, there is a difference of helicity injection ratio between the toroidal and poloidal directions by more than several times. In addition, relative helicity and relative ohmic injection ratios are thought to be small to change the global plasma behavior considerably. Of course the direct arc with the shortest path between two plates can be excluded because of the observed (localized but global) effects on the plasma properties.

The first possibility to account for the plasma response in this experiment is that the current path

does not obey accurately the mean magnetic field line such as in the model proposed by Rusbridge [32]. This model may describe the same effective current flow even if we change the current injection angle. However, other RFP experiments might have shown markedly different results if the Rusbridge model was employed. For example, the electron high heat flux near the plasma edge with the larger magnetic field fluctuations, commonly observed in RFPs, may not be unidirectional according to this model.

The second possibility is the increased conductivity due to the edge heating by this forced current. At least significant edge heating may not occur because the injected current increases smoothly with time: the effective electrical circuit values can be expressed as time constant ones mentioned before (see Fig. 9). If the resistance R_H becomes half of 15mΩ, *i.e.*, R is from 95mΩ to 80mΩ, changes of I_H and V_H at $t \sim 0.65$ms are 0.45kA (+ 10%) and − 70V (− 28%), respectively.

The third possibility is a trigger to change the equilibrium by this injection, *e.g.*, from one MHD stability region to another. This means, for example, that the relaxation phenomena may be expected to allow various angles of helicity (current) injection to cause the same plasma behavior. The helicity injection requires a directivity with respect to the magnetic field line but the energy injection does not. Therefore, the experimental results suggest that the energy injection is more important than the helicity injection; Locally near the injection port, the relative ohmic injection rate may be larger than a few tens of %. By this injection, an excess magnetic energy decreases rapidly than the helicity changes, and the plasma may take the more relaxed state locally [1,5]. According to Kondoh *et al.*[33], the plasma takes the relaxed state considering the attractor of the dissipative structure in the resistive MHD plasma. Their theory can explain our results of relaxation phenomena, which may be affected by the injection of the energy not by the helicity.

We apply a voltage between two separate conductive electrodes (type D and nearly the same single disk with type C) with an insulation on one surface. These are located on $\Delta\phi = 140°$ toroidally away each other. This setup is recommended in order to have the higher impedance Z [9], but we do not observe the appreciable change of plasma parameters in this configuration.

These obtained results including R_H and L_H values discussed before, indicate that the injected current path is localized near the injection port and then the current is lost by touching the wall near the injection port. In order to demonstrate this helicity injection scheme more clearly and globally around the torus, the number of the injection port and the local current density must be increased. Designing a more efficient injection probe with less affecting the plasma-probe interaction is also required for future.

4. Conclusions

Using various kinds of movable limiter and injection probe for edge dissipation study, changes of plasma parameters are studied in the REPUTE-1 RFP device. With an advance of the material into the plasma, monotonic increases in the loop voltage V_l and magnetic fluctuations (especially HF part) are found with an increasing rate dependent on the shape of limiters. On the other hand, gradual decreases in H_α, soft X-ray and CV intensities as well as the central electron temperature T_e are observed. Nearly constant ion temperature T_i derived from CV line regardless of the insertion depth of D is also obtained. Drastic increases in V_l and I_{sx} $(a/4)$ intensity are found as the material is beyond a certain position of $D \sim 8$cm. The V_l increase is examined and discussed comparing with theories based on the Spitzer resistivity and helicity balance. The voltage increase can be explained mainly by the effective reduction of the plasma size, using Spitzer resistivity. The induced voltage between two parallel plates is also measured (< 60V) as a function of D, which reflects the presence of the high energy electrons (at least more than 20eV with a relative population of less than several %) from the estimation.

Next, effects on plasma performance are studied by the dc helicity injection for the first time, applying a voltage between two parallel plates inserted into the plasma edge ($D \sim 5$cm). The current I_H up to 9kA is nearly proportional to the applied voltage V_H. A transient increase in the toroidal flux by $\sim 10\%$ and a gradual decrease in

the edge poloidal field by $< 10\%$ (plasma takes the more relaxed state) is found near the injection port, regardless of the polarity of V_H. An analysis of the electrical circuit is also done to estimate the load of the probe part. The enhanced impurity line intensities of CV and OV (also soft X-ray intensities) or a degradation of plasma performance are not observed.

Acknowledgements

The author wishes to acknowledge the continuous encouragement of Prof. H. Toyama. He is also grateful to K. Yamagishi, T. Oikawa and the REPUTE-1 group for operating this device during experiments. This work has been partly supported by a Grant-in Aid for Scientific Research from the Ministry of Education, Science and Culture, Japan.

References

[1] H. A. B. Bodin, Nucl. Fusion **30**, 1717 (1990).
[2] A. Fujisawa, H. Ji, K. Yamagishi, S. Shinohara, H. Toyama and K. Miyamoto, Nucl. Fusion **31**, 1443 (1991).
[3] T. Ohkawa, Nucl. Fusion **10**, 1335 (1970).
[4] N. Fisch, Phys. Rev. Lett. **41**, 873 (1978).
[5] J. B. Taylor, Phys. Rev. Lett. **33**, 1139 (1974).
[6] M. Ono, G. J. Greene, D. Darrow, C. Forest, H. Park and T. H. Stix, Phys. Rev. Lett. **59**, 2165 (1987).
[7] K. F. Schoenberg, J. C. Ingraham, C. P. Munson, P. G. Weber, D. A. Baker, R. F. Gribble, R. B. Howell, G. Miller, W. A. Reass, A. E. Schofield, S. Shinohara and G. A. Wurden, Phys. Fluids **31**, 2285 (1988).
[8] J. B. Taylor and M. F. Turner, Nucl. Fusion **29**, 219 (1989).
[9] Y. L. Ho, Nucl. Fusion **31**, 341 (1991).
[10] S. Shinohara, Plasma Phys. Control. Fusion **35**, 1661 (1993).
[11] P. C. Stangeby and G. M. McCracken, Nucl. Fusion **30**, 1225 (1990).
[12] B. Alper and H. Y. W. Tsui, *Proc. of the 14th Europ. Conf. on Control. Fusion and Plasma Phys. 1987* (European Physical Society, Madrid, Spain, 1987), Vol.11D, Part II, p.434.
[13] P. G. Carolan, A. R. Field, A. Lazaros, M. Rusbridge, H. Y. W. Tsui and M. K. Bevir, *Proc. of the 14th Europ. Conf. on Control. Fusion and Plasma Phys. 1987* (European Physical Society, Madrid, Spain, 1987), Vol.11D, Part II, p.469.
[14] H. Y. W. Tsui, Nucl. Fusion **28**, 1543 (1988).
[15] S. Shinohara, I. Ueda, M. Awano, Y. Shimazu, A. Fujisawa, H. Ji, A. Ejiri, A. Shirai, S. Odachi, K. Mayanagi, K. Yamagishi, H. Toyama and K. Miyamoto, *Proc. of the 17th Europ. Conf. on Control. Fusion and Plasma Heating 1990* (European Physical Society, Amsterdam, Netherlands, 1990), Vol.14B, Part II, p.541.
[16] P. G. Weber, J. C. Ingraham, R. F. Ellis, G. A. Wurden, C. P. Munson and J. N. Downing, Phys. Fluids **B3**, 1701 (1991).
[17] S. Shinohara, S. Ohdachi, H. Toyama, K. Miyamoto and T. Banno, Phys. Fluids **B5**, 464 (1993).
[18] T. R. Jarboe and B. Alper, Phys. Fluids **30**, 1177 (1987).
[19] A. R. Jacobson and R. W. Moses, Phys. Rev. Lett. **52**, 2041 (1984).
[20] N. Asakura, T. Fujita, K. Hattori, N. Inoue, S. Ishida, Y. Kamada, S. Matsuzuka, K. Miyamoto, J. Morikawa, Y. Nagayama, H. Nihei, S. Shinohara, H. Toyama, Y. Ueda, K. Yamagishi and Z. Yoshida, Plasma Phys. Control. Fusion **28**, 805 (1986).
[21] S. Shinohara, K. Yamagishi, S. Ohdachi, A. Ejiri, K. Mayanagi, Y. Shimazu and K. Miyamoto, Plasma Phys. Control. Fusion **34**, 627 (1992).
[22] S. Shinohara, K. Yamagishi, S. Ohdachi, A. Ejiri, H. Toyama and K. Miyamoto, J. Phys. Soc. Jpn. **61**, 3030 (1992).
[23] J. C. Ingraham, R. F. Ellis, J. N. Downing, C. P. Munson, P. G. Weber and G. A. Wurden, Phys. Fluids **B2**, 143 (1990).
[24] Y. Yagi, Y. Hirano, T. Shimada, K. Hattori, Y. Maejima, I. Hirota and A. A. Newton, Plasma Phys. Control. Fusion **33**, 1391 (1991).
[25] H. Ji, H. Toyama, A. Fujisawa, S. Shinohara and K. Miyamoto, Phys. Rev. Lett. **69**, 616 (1992).
[26] T. Asakura, Master's thesis, University of Tokyo, 1992.
[27] K. Shimano, Master's thesis, University of Tokyo, 1993.
[28] N. Asakura, Y. Nagayama, S. Shinohara, H. Toyama and K. Miyamoto, Nucl. Fusion **29**, 893 (1989).
[29] H. Ji, H. Toyama, K. Yamagishi, S. Shinohara, A. Fujisawa and K. Miyamoto, Rev. Sci. Instrum. **62**, 2326 (1991).
[30] A. Fujisawa and K. Miyamoto, J. Phys. Soc. Jpn. **58**,

473 (1989).

[31] H. Toyama, H. Ji, A. Ejiri, T. Yoshikawa, Y. Shimazu, T. Asakura, M. Awano, A. Fujisawa, S. Ohdachi, T. Oikawa, K. Shimano, K. Shinohara, S. Shinohara, K. Yamagishi, K. Miyamoto, Z. Yoshida, S. Kido, Y. Ogawa, H. Nihei, J. Morikawa, S. Takeji, J. Uchikado, K. Sasaki, M. Watanabe, H. Nakanishi, Y. Yamakoshi and N. Inoue, *Plasma Phys. and Control. Nucl. Fusion Research 1992*, Würzburg (International Atomic Energy Agency, Vienna, 1993), Vol.2, p.547.

[32] M. G. Rusbridge, Nucl. Fusion **22**, 1291 (1982).

[33] Y. Kondoh, Y. Hosaka and J. L. -Liang, National Institute for Fusion Science, Research Report No.NIFS-212, 1993.